Membrane and Water Treatment, *Vol. 12, No. 2 (2021) 59-64*
DOI: https://doi.org/10.12989/mwt.2021.12.2.059

Performance prediction of flat sheet commercial nanofiltration membrane using Donnan-Steric Pore Model

Danial Qadir*[1], Rizwan Nasir[2], Hilmi Mukhtar[1] and Fahim Uddin[3]

[1]Department of Chemical Engineering, University Teknologi PETRONAS, Sri Iskandar, 32610, Perak, Malaysia
[2]Department of Chemical Engineering, University of Jeddah, Asfan Road, 23890, Jeddah, Saudi Arabia
[3]Department of Chemical Engineering, NED University of Engineering and Technology, University Road, 75270, Karachi, Pakistan

(Received November 5, 2020, Revised March 1, 2021, Accepted March 14, 2021)

Abstract. The rejection of sodium chloride (NaCl) and calcium chloride ($CaCl_2$) single salt solutions were carried out for commercial nanofiltration NFDK membrane. Results showed that the NFDK membrane had a negative surface charge and had a higher observed rejection of 93.65% for calcium (Ca^{2+}) ion and 78.27% for sodium (Na^+) ions. Prediction of rejection for aqueous solutions of both salts was made using Donnan Steric Pore Model based on Extended Nernst-Planck Equation in addition to concentration polarization film theory. A MATLAB program was developed to execute the model calculations. Absolute Average Relative Error (% AARE) was found below 5% for real rejection of the NFDK membrane. This research could be used successfully to assess the membrane characterization parameter using a proposed procedure which can reduce the number of experiments.

Keywords: donnan-steric partitioning model; flat sheet; nanofiltration; Nernst Planck equation; real rejection

1. Introduction

Numerous technologies have been developed in the last decade to treat or purify the water. Reverse osmosis (RO), ultrafiltration (UF), Microfiltration (MF), and nanofiltration are the most important membrane-based water technologies (Khulbe *et al.* 2012). The nanofiltration membrane has intermediate separation efficiency between ultrafiltration (UF) and reverse osmosis (RO). The asymmetric polymeric NF membranes consist of a low resistance support layer with a functionally active porous top layer with 1nm pore size diameter and fixed charges. Due to these features, NF membranes retain multivalent complex ions and permeate small uncharged solutes and low charged ions. Nanofiltration membranes generally possess the charged surfaces either positive or negative because of dissociation of membranes' functional groups or charged species adsorption from solution (Fang and Deng 2014, Labban *et al.* 2017).

The separation mechanisms for NF include a steric exclusion for neutral species or steric and charge exclusion (between inorganic species and membranes). Other likely mechanisms could be diffusivity, solubility, differences in Born self-energy, and dielectric exclusion (Labban *et al.* 2017, Shahbabaei and Kim 2017). Consequently, different models have been proposed over the years to predict the rejection of NF membranes. Earlier models were developed based on Spiegler and Kedem's work considering the membranes of a black-box model. This model was meant for dense membranes but had been used to evaluate nanofiltration membranes. Since this model does not provide any information about the membrane's structural and electrical properties, it cannot be used for prediction purposes (Agboola *et al.* 2014, Wang *et al.* 2016). For such reasons, the modified, extended Nernst Planck models were introduced, allowing the evaluation of membrane charge.

Furthermore, the Extended Nernst Planck equation-based DSPM model was reasonable to predict the nanofiltration membranes (Wang *et al.* 2014). This module included electroneutrality condition in the membrane, and ion partitioning on membrane interfaces was described by Donnan equilibrium with steric effects. The accurate portrayal of NF membrane separation is multifaceted and depends on micro-hydrodynamics and interfacial events occurring at the membrane surface and in membrane pores (Wang *et al.* 2014, Wang *et al.* 2016).

In this work, the rejection of commercial flat sheet nanofiltration membrane NFDK is investigated. Rejection of single salt aqueous NaCl and $CaCl_2$ of different concentrations were evaluated for the NFDK membrane. Prediction of sodium (Na^+) and calcium (Ca^{2+}) were determined using a self-developed MATLAB program depending on DSPM with the concentration polarization film theory model. To the author's best knowledge, no studies have been made to calculate the model parameters and dominant transport mechanisms using the built-in MATLAB functions that could also reduce the number of experiments.

1.1 Theoretical background

The subsequent assumptions are used for the mathematical modeling of the DSPM model (Szymczyk *et al.* 2003):

---

*Corresponding author, Ph.D.
E-mail: danial2715@gmail.com

http://www.techno-press.org/?journal=mwt&subpage=7

ISSN: 2005-8624 (Print), 2092-7037 (Online)

Table 1 Equation for DSPM model (Wang *et al.* 2014)

Parameters	Equations
Concentration Gradient	$\frac{dc_i}{dx} = \frac{J_v}{D_{ip}}\left(K_{ic}c_i - C_{ip}\right) - \left(\frac{Z_i c_i F}{RT}\frac{d\psi}{dx}\right)$
Potential Gradient	$\frac{d\psi}{dx} = \frac{\left[\sum_{i=1}^{n} z_i \frac{J_v}{D_{ip}}\left(K_{ic}c_i - c_{ip}\right)\right]}{\left[\frac{F}{RT}\sum_{i=1}^{n}\left(z_i^2 c_i\right)\right]}$
Donnan-Steric Partitioning	$\frac{c_i}{C_i^o} = \varphi\, exp\left(-\frac{z_i F}{RT}\Delta\psi_d\right)$
Hindrance Factors	$K_{id} = -1.705\lambda + 0.946$ $K_{ic} = -0.301\lambda + 1.022$
Electroneutrality Conditions	$\sum_{i=1}^{n} z_i c_i + X = 0$ (Inside Membrane) $\sum_{i=1}^{n} z_i C_i = 0$ (Bulk Solution)
Concentration Polarization Film Theory	$\frac{(C_{im} - C_{ip})}{(C_{ib} - C_{ip})} = e^{Jv/k}$

i. The membrane consists of cylindrical pores of r_p and length Δx.

ii. Effective membrane charge (X) is constant throughout the membrane, and it depends on feed concentration only. It can be expressed in Freundlich isotherm, and solution properties are presented in equivalent/m^3.

Iii. The excess solvent is present, and no coupling between electrolyte components is existent in the solution. Hence the difference in average velocities between them is negligible.

iv. Radially averaged values for molar fluxes, concentrations, electric potential are considered.

v. Hagen-Poiseuille type fully developed flow is present in membrane pores.

The basic set of equations used in the DSPM model are tabulated in Table 1 here.

2. Experimentation

2.1 Materials

The reagent grade Sodium Chloride (NaCl) and Calcium Chloride (CaCl$_2$) salts were obtained from R & M chemicals Ltd. to study the membrane's rejection capability. Commercial Flat sheet nanofiltration membrane NFDK was bought from GE Osmonics. The primary characteristics of the NFDK membrane are highlighted in Table 2.

2.1 Methods

2.1.1 Morphology of membrane

NFDK membranes' morphology was evaluated using the Variable Pressure Scanning Electron Microscope (VPFESEM, Zeiss Supra55 VP). Moreover, the structural information was assessed through FESEM analysis.

Table 2 Basic information of membrane and their characteristics

Membrane Code	MWCO	pH Range	MgSO$_4$ Rejection	Permeability m^3/ (m^2.s. kPa)	Contact Angle
NFDK	150-300	2-11	98%	7.96 E^{-9}	50.2

2.1.2 Compaction of membrane and Pure Water Flux (PWF)

The compaction of the NFDK membrane was completed at 14 bar transmembrane pressure. Water was collected gravimetrically until constant flux was achieved. The NFDK PWF was determined at a pressure range from 2 to 10 bar. The water permeate was collected through the gravimetric method by weighing the mass of water collected at a predetermined time.

2.1.3 Rejection of solutes

The rejection of solutes was determined by measuring the electrical conductivity (EC) of permeate and feed solutions. 25 ml of permeate sample was collected for each transmembrane pressure at 350 rpm. Permeate flux was measured using the gravimetric method. Aqueous solutions of both salts were prepared at 100 ppm concentrations. The rejection was performed for both salts from 2 bar to 10 bar with 2 bar increments. No pH adjustments were made for aqueous solutions. The effect of concentration polarization was also added to the model by using the film theory model. Moreover, calibration curves were drawn to correlate ions' electrical conductivity in an aqueous solution to its concentration. This relation was then used to measure the concentration of ion permeate and feed solutions for each sample collected.

2.2 Experimental set-up

The Sterlitech stirred dead-end filtration cell (HP-4750) was used to evaluate NFDK flat sheet membranes' performance. A circular membrane with a 50 mm diameter with 14.6 cm^2 active surface area was used for testing. The desired pressure in the filtration cell was created with nitrogen gas. The conductivity meter by HANNA was used to measure the ion concentration in permeate.

2.3 Model calculations

The Donnan Steric pore model was used to evaluate the membrane's rejection ability for single electrolyte solutions. Since solutions are considered dilute, the coupling is nonexistent. Also, membrane pores are large enough to ignore the dielectric interactions. The model calculation procedure is followed as given in (Lee and Lueptow 2001). Three parameters, such as effective pore radius (r_p), effective membrane charge density (X), and effective membrane thickness to porosity ratio ($\Delta x/A_k$) were determined through the MATLAB program. An initial guess range of X, r_p, and ($\Delta x/A_k$) was provided to start the calculation. Interface concentrations were determined using *fsolve*, considering c_{im} equal the c_{ip}, which are both feed side and permeate side membrane interface concentrations,

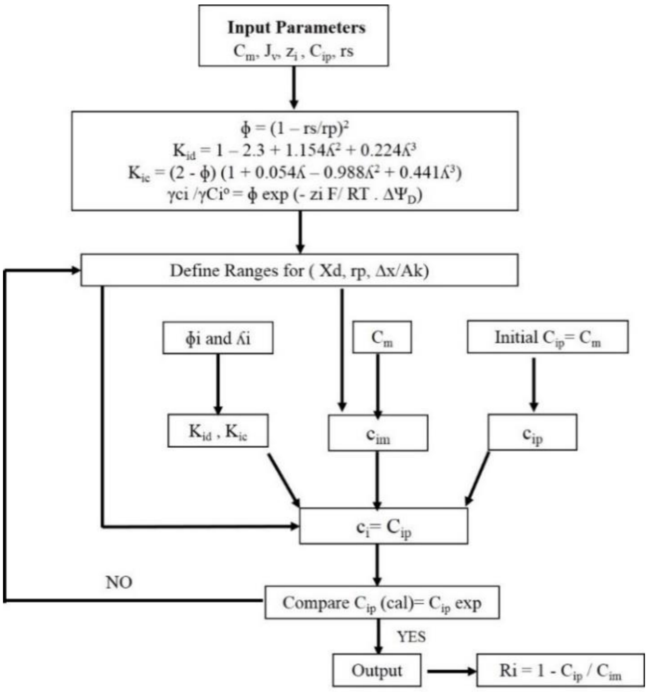

Fig. 1 Schematic diagram of a numerical procedure to calculate the membrane structural parameter using the Donnan Steric pore model

respectively. Permeate concentration in permeate (C_{ip}) was calculated using *bvp4c* functions in MATLAB. The difference was minimized through global minimization function *patternsearch* until *AARE (%)* was minimized within 5%.

3. Results and discussion

3.1 Morphological analysis

The FESEM micrograph of the NFDK membrane showed a membrane thickness of 131 μm. The membrane top selective thickness layer was taken from Fong *et al.* and found to be 2.66 μm, and the mean pore diameter of the membrane was reported to be 0.388 nm (Fang and Deng 2014). The selective layer is the one that controls the rejection of solutes and flux of solvent. Fig. 2 represents the FESEM image of NFDK membrane studies in this work.

3.2 Performance analysis

3.2.1 Pure Water Flux (PWF)

The PWF was studied at 2-10 bar pressure with an interval of 2 bar; the permeate volume was collected from the bottom of the filtration cell after 10 min. The PWF was calculated using Eq. (1)

$$J = \frac{V}{A\Delta t} \tag{1}$$

where J, V, A, and Δt are notations for flux, volume collected, membrane effective area, and time respectively.

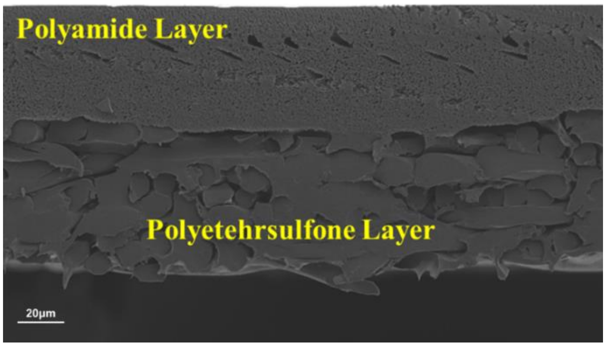

Fig. 2 Cross-section (FESEM image) of NFDK flat sheet membrane

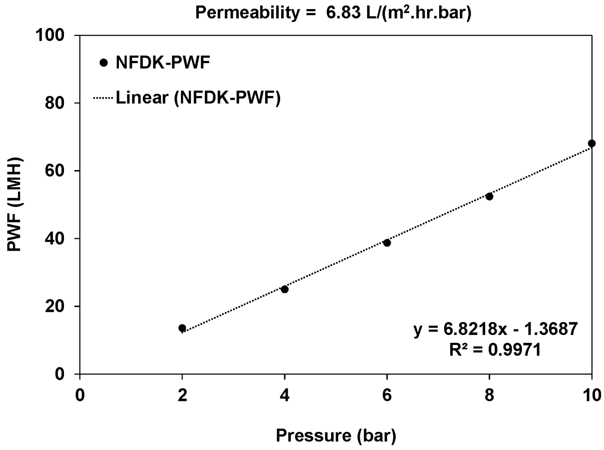

Fig. 3 Pure water flux of NFDK flat sheet membrane

Fig. 3 represents the PWF of NFDK as a function of pressure. The plot's slope gives the water permeability, which permits calculating the $r_p^2/(\Delta x/A_k)$ through the Hagen-Poisuille equation. Hence, considering the r_p value equal to 1 nm as an initial guess value, effective membrane thickness to porosity ratio ($\Delta x/A_k$) could be estimated to solve the model. Water permeability of the NFDK membrane was found to be 6.83 L/(m^2.hr.bar), which falls in the range of permeability (3.1-7.9) L/(m^2.h.Bar) reported in the literature (Bargeman *et al.* 2014) for this membrane.

3.2.2 Permeate flux

An investigation of permeate fluxes of 100 ppm aqueous solutions of both salts reveals that aqueous solution containing sodium salt had better permeate flux than that of calcium salt, as shown in Fig. 4. It was observed that both salts exhibited an increasing trend with the increase in pressure. It was also noted that NaCl has a higher flux than $CaCl_2$ at a similar concentration. The concentration polarization layer over the membrane surface due to ions' rejection is the main reason for the better permeate flux. Since calcium ions have bigger stoke radii than sodium ions, it could be deduced that the concentration polarization layer's development occurred quickly for calcium salt, and subsequently, permeate flux dropped.

Such a trend has been extensively observed in the literature (Ferreira Esmi *et al.* 2013, Fang and Deng 2014, Jadhav *et al.* 2016). Recently, the NaCl and sodium arsenate

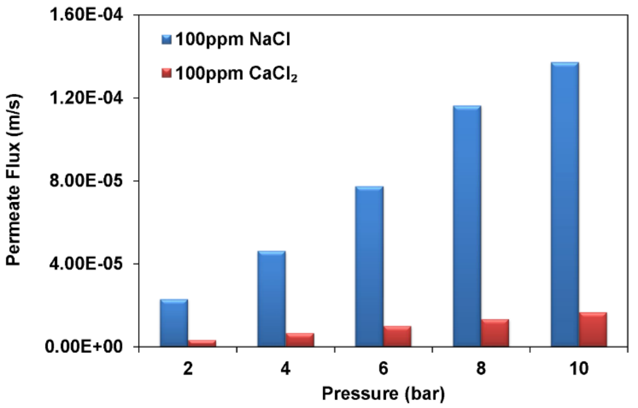

Fig. 4 Permeate fluxes of 100 ppm NaCl and $CaCl_2$ aqueous solution for NFDK nanofiltration membrane

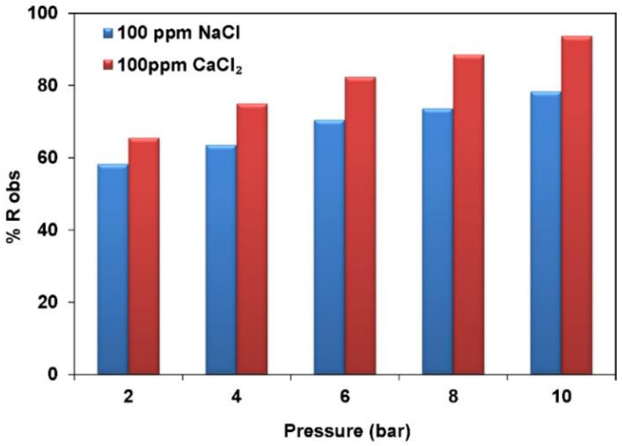

Fig. 5 Observed rejection of 100 ppm aqueous solutions of NaCl and $CaCl_2$ salts for NFDK membrane

aqueous solution through NFDK membrane has been studied by Fang *et al*. They observed the reduced permeate flux for sodium arsenate solution. They argued that the development of concentration polarization halted the transport of solvent ions through the membrane resulting in lower flux (Fang and Deng 2014). Also, previous studies confirm a similar trend of permeate flux w.r.t. pressure. Kaykioglu *et al*. studied the nanofiltration membranes for the treatment of wastewater from the textile industry. They also found the same trend of permeate flux w.r.t. pressure (Kaykioglu *et al*. 2017).

3.2.2 Rejection studies

The observed rejection of NFDK was estimated by filtering the model solutions of sodium chloride and calcium chloride of 100 ppm concentration. Eq. (2) was used to calculate the observed rejection, where C_p and C_f denote permeate and feed concentrations, respectively (Li *et al*. 2004, Abdel-Fatah *et al*. 2020).

$$R_{obs}(\%) = (1 - C_p/C_f) \times 100 \tag{2}$$

The following relation calculated real rejection of the NFDK membrane

$$R_{real}(\%) = (1 - C_{ip}/C_f) \times 100 \tag{3}$$

Concentration polarization at the membrane surface was included in the model to correlate the observed and real rejection by using the following equation

$$\ln\left[(1-R_{obs})/R_{obs}\right] = \ln\left[(1-R_{real})/R_{real}\right] + J_v/k \tag{4}$$

where m (slope of this equation)=$1/k'$. Hence, by using the mass transfer coefficient for the dead-end cell can be determined by using the following relation

$$k = k'w^{0.567} \tag{5}$$

Here "w" denotes the stirring speed of the dead-end filtration cell.

Observed rejection (% R_{obs}) of 100 ppm aqueous sodium chloride and calcium chloride salts is depicted in Fig. 5. It can be deduced that the observed rejection of both salts increased with the increase in feed pressure. The rejection is much influenced by pressure as reported by (Kheriji *et al*. 2016). Observed rejection for NaCl solution varied from 58.2% to 78.27% while for $CaCl_2$ solution, it raised to 93.65% from 65.5%. It is a general trend for single salt rejection through nanofiltration membranes since with the increase in pressure, more solvent transports through the membrane due to increased pressure gradient. Albeit, solute molecules are hindered owing to membrane charge and their steric hindrance (Labbez *et al*. 2003). Fig. 5 illustrates that the rejection of calcium salt exceeded that of sodium salt. According to the Donnan Exclusion mechanism, the higher valence of counter ion leads to lower rejection if co-ions are the same for both salts (Pérez-González *et al*. 2015, Qadir *et al*. 2017).

Since the reverse order is found in this study, some other rejection mechanisms must be in play. The hypothesis could explain this reversal of rejection order that ions with lower diffusivity or bigger size could be hindered more than their counterparts, causing an increase in rejection (Labbez *et al*. 2002). Since Ca^{2+} ion is bigger (stokes Radius: 0.310 nm) than Na^+ ion (stokes radius: 0.184 nm) and has less diffusivity (D_{Ca}=0.92×10^{-9} m^2/s<D_{Na}=1.33×10^{-9} m^2/s), it is retained better than its competitive ion i.e., Na^+, hence resulting in better rejection for calcium chloride salt. Labbez *et al*. have mentioned this reverse trend of single salt solutions. They found that $MgCl_2$ was better retained than NaCl aqueous solution. They attributed this result to the adsorption of ion on the membrane surface, causing this reversal order in contrast to general observations for nanofiltration membranes (Labbez *et al*. 2003).

3.3 Model calculations

The modeling results of the NFDK membrane for sodium chloride and calcium chloride of 100 ppm aqueous solutions are shown in Figs. 6 and 7. Solid lines are real rejections calculated by the model, and data points are the real rejections calculated through experimentally based calculations. Real rejection is found to be the function of permeate flux as it generally occurs for negatively charged commercial nanofiltration membranes. It also revealed that Donnan Steric partitioning did not play a dominant role during the rejection rather diffusivities. The respective ions'

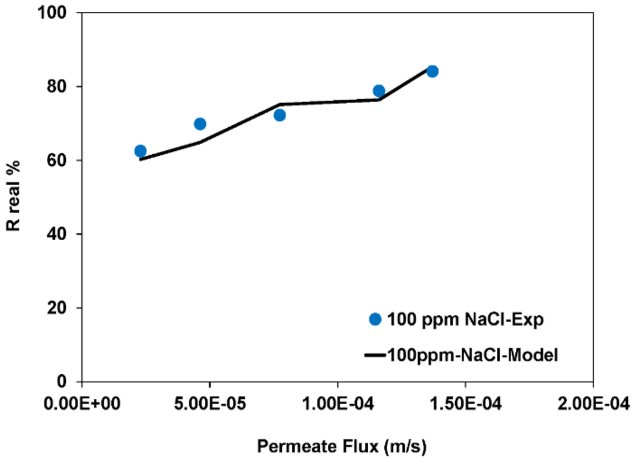

Fig. 6 Real rejection as a function of permeate flux for 100 ppm aqueous solutions of NaCl by NFDK membrane

steric hindrances controlled the separation mechanism since calcium salt was unexpectedly highly rejected than sodium salt.

Values of membrane parameters such as r_p, X, and ($\Delta x/A_k$) solved by MATLAB program are 0.44 nm, 2.65 μm, and -189.20 mol/m^{3,} respectively. It is found that the new approach of finding membrane characterization parameters through the global minimization function could be an excellent tool to reduce the number of experiments. Moreover, experimental data is in good agreement with the DSPM model in conjuncture with the concentration polarization film theory. %AARE was about 1% for NaCl and about 3% for $CaCl_2$, supporting this new approach to solving the membrane's structural parameters.

4. Conclusions

The performance of a flat sheet commercial nanofiltration membrane (NFDK) was evaluated and then modeled using the DSPM model. The NFDK membrane showed higher rejection for $CaCl_2$ aqueous solution than NaCl based aqueous solution. The membrane did not show the typical behavior of commercial NF membranes since Donnan exclusion did not play a dominant role in the rejection of solute ions; instead, electrolytes controlled the mechanism based on their inherent characteristics such as size and diffusivities. An excellent agreement was found between the model and experimental values of rejection using the MATLAB program, which could be successfully employed to determine membranes' structural parameters instead of running the excessive number of experiments and through tiresome fitting procedures.

Acknowledgments

The authors are thankful to the MyRA funding authority for financial support (0153AB-J16) and Universiti Teknologi PETRONAS, Malaysia, for the technical support and lab facilities.

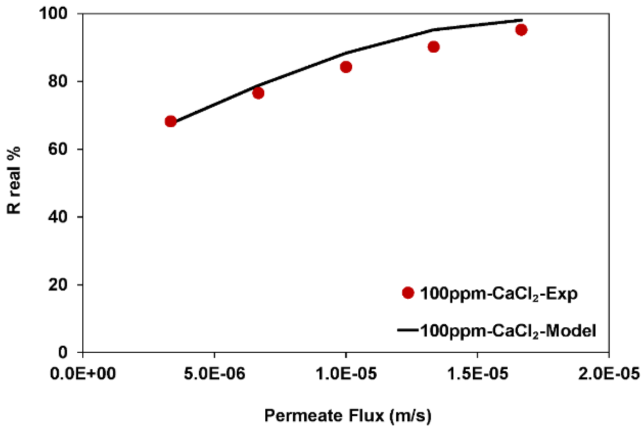

Fig. 7 Real rejection as a function of permeate flux for 100 ppm aqueous solutions of $CaCl_2$ by NFDK membrane

References

Abdel-Fatah, M.A., Khater, E., Hafez, A. and Shaaban, A. (2020), "Performance of fouled NF membrane as used for textile dyeing wastewater", *Membr. Water Treat.*, **11**(2), 111-121. https://doi.org/10.12989/mwt.2020.11.2.111.

Agboola, O., Maree, J. and Mbaya, R. (2014), "Characterization and performance of nanofiltration membranes", *Environ. Chem. Lett.*, **12**(2), 241-255. https://doi.org/10.1007/s10311-014-0457-3.

Bargeman, G., Westerink, J.B., Guerra Miguez, O. and Wessling, M. (2014), "The effect of NaCl and glucose concentration on retentions for nanofiltration membranes processing concentrated solutions", *Sep. Purif. Technol.*, **134**, 46-57. https://doi.org/10.1016/j.seppur.2014.07.025.

Fang, J. and Deng, B. (2014), "Arsenic rejection by nanofiltration membranes: Effect of operating parameters and model analysis", *Environ. Eng. Sci.*, **31**(9), 496-506. https://doi.org/10.1089/ees.2013.0460.

Fang, J. and Deng, B. (2014), "Rejection and modeling of arsenate by nanofiltration: Contributions of convection, diffusion and electromigration to arsenic transport", *J. Membr. Sci.*, **453**, 42-51. http://doi.org/10.1016/j.memsci.2013.10.056.

Ferreira Esmi, C., Schrive, L., Barre, Y., Palmeri, J. and Deratani, A. (2013), "Using nanofiltration in a "zero-rejection" process: The removal of Ni^{2+} and Co^{2+} from salty wastewater", *Desalin. Water Treat.*, **51**(1-3), 476-484. https://doi.org/10.1080/19443994.2012.714526.

Jadhav, S.V., Marathe, K.V. and Rathod, V.K. (2016), "A pilot scale concurrent removal of fluoride, arsenic, sulfate and nitrate by using nanofiltration: Competing ion interaction and modelling approach", *J. Water Proc. Eng.*, **13**, 153-167. http://doi.org/10.1016/j.jwpe.2016.04.008.

Kaykioglu, G., Ata, R., Tore, G.Y. and Agirgan, A.O. (2017), "Evaluation of effects of textile wastewater on the quality of cotton fabric dye", *Membr. Water Treat.*, **8**(1), 1-18. https://doi.org/10.12989/mwt.2017.8.1.001.

Kheriji, J., Tabassi, D., Bejaoui, I. and Hamrouni, B. (2016), "Boron removal from model water by RO and NF membranes characterized using SK model", *Membr. Water Treat.*, **7**(3), 193-207. http://doi.org/10.12989/mwt.2016.7.3.193.

Khulbe, K., Feng, C., Matsuura, T. and Ismail, A. (2012), "Progresses in membrane and advanced oxidation processes for water treatment", *Membr. Water Treat.*, **3**(3), 181-200. https://doi.org/10.12989/mwt.2012.3.3.181.

Labban, O., Liu, C., Chong, T.H. and Lienhard, V.J.H. (2017), "Fundamentals of low-pressure nanofiltration: Membrane characterization, modeling, and understanding the multi-ionic interactions in water softening", *J. Membr. Sci.*, **521**, 18-32. http://doi.org/10.1016/j.memsci.2016.08.062.

Labbez, C., Fievet, P., Szymczyk, A., Vidonne, A., Foissy, A. and Pagetti, J. (2002), "Analysis of the salt retention of a titania membrane using the "DSPM" model: Effect of pH, salt concentration and nature", *J. Membr. Sci.*, **208**(1-2), 315-329. http://doi.org/10.1016/S0376-7388(02)00310-1.

Labbez, C., Fieve, P., Szymczyk, A., Vidonne, A., Foissy, A. and Pagetti, J. (2003), "Retention of mineral salts by a polyamide nanofiltration membrane", *Sep. Purif. Technol.*, **30**(1), 47-55. http://doi.org/10.1016/S1383-5866(02)00107-7.

Lee, S. and Lueptow, R.M. (2001), "Membrane rejection of nitrogen compounds", *Environ. Sci. Tech.*, **35**(14), 3008-3018. https://doi.org/10.1021/es0018724.

Li, D., Chung, T.S., Ren, J. and Wang, R. (2004), "Thickness dependence of macrovoid evolution in wet phase-inversion asymmetric membranes", *Ind. Eng. Chem. Res.*, **43**(6), 1553-1556. https://doi.org/10.1021/ie034264g.

Pérez-González, Ibáñez, A., R., Gómez, P., Urtiaga, A.M., Ortiz, I. and Irabien, J.A. (2015), "Nanofiltration separation of polyvalent and monovalent anions in desalination brines", *J. Membr. Sci.*, **473**, 16-27. https://doi.org/10.1016/j.memsci.2014.08.045.

Qadir, D., Mukhtar, H. and Keong, L.K. (2017), "Retention of sulfate and chloride ions in commercially available tubular membranes", *Membr. Water Treat.*, **8**(4), 369-380. https://doi.org/10.12989/mwt.2017.8.4.369.

Shahbabaei, M. and Kim, D. (2017), "Molecular simulation study of water transport through aquaporin-inspired pore geometry", *J. Mech. Sci. Tech.*, **31**(8), 3845-3851. https://doi.org/10.1007/s12206-017-0729-5.

Szymczyk, A., Labbez, C., Fievet, P., Vidonne, A., Foissy, A. and Pagetti, J. (2003), "Contribution of convection, diffusion and migration to electrolyte transport through nanofiltration membranes", *Adv. Colloid. Interfac.*, **103**(1), 77-94. http://doi.org/10.1016/S0001-8686(02)00094-5.

Wang, J., Dlamini, D.S., Mishra, A.K., Pendergast, M.T.M., Wong, M.C.Y., Mamba, B.B., Frege,r V., Verliefde, A.R.D. and Hoek, E.M.V. (2014), "A critical review of transport through osmotic membranes", *J. Membr. Sci.*, **454**, 516-537. http://doi.org/10.1016/j.memsci.2013.12.034.

Wang, J., Mo, Y., Mahendra, S. and Hoek, E.M.V. (2014), "Effects of water chemistry on structure and performance of polyamide composite membranes", *J. Membr. Sci.*, **452**, 415-425. http://doi.org/10.1016/j.memsci.2013.09.022.

Wang, L., Dumont, R.S. and Dickson, J.M. (2016), "Molecular dynamic simulations of pressure-driven water transport through polyamide nanofiltration membranes at different membrane densities", *RSC Adv.*, **6**(68), 63586-63596. http://doi.org/10.1039/C6RA12115B.

CC

Nomenclature

c_i	Concentration in the membrane (mol m^{-3})
C_{ip}	Concentration in permeate (mol m^{-3})
C_{ib}	Concentration in the bulk solution (mol m^{-3})
D_{ip}	Hindered diffusivity (m^2 sec^{-1})
F	Faraday constant (C mol^{-1})
J_v	Permeate flux (L m^{-2} h^{-1})
$K_{i,c}$	Hindrance factor for convection
K_{id}	Hindrance factor for diffusion
R	Gas constant (J mol^{-1} K^{-1})
T	Absolute temperature (K)
w	Stirring speed of the dead-end filtration cell.
X	Effective membrane charge density
Z_i	Valence of ion
$\Delta\psi_d$	Donnan potential (V)
φ	Steric hindrance factor
λ	Ionic radius to pore radius ratio